Supporting information for the article:

Probing the Interaction of Quantum Dots with Chiral Capping Molecules using Circular Dichroism Spectroscopy

Assaf Ben-Moshe,[1‡] Ayelet Teitelboim,[2‡] Dan Oron,[2] Gil Markovich[1*]*

[1] School of Chemistry, Raymond and Beverly Sackler Faculty of Exact Sciences, Tel Aviv University, Tel Aviv 6997801, Israel.

[2] Department of Physics of Complex Systems, Weizmann Institute of Science, Rehovot 7610001, Israel

* G. Markovich, email: gilmar@post.tau.ac.il, D. Oron, email: dan.oron@weizmann.ac.il

Experimental methods

Chemicals: L-cysteine (98.5%), sodium hydroxide (ACS reagent 97%), oleic acid (OA), cadmium oxide (99.99%), octadecylamine (ODA, 97%), selenium (99.999%), sulfur (99.5%), tri-n-octylphophine (TOP, 90%), octylamine (97%), octadecene (ODE, 90%) and organic solvents were purchased from Sigma Aldrich. Trioctylphophine oxide (TOPO, 97%) from STREM chemicals. Tetradecylphosphonic acid (TDPA) and octadecylphosphonic acid (ODPA) from PCI synthesis, All chemicals were used without further purification.

Synthesis of CdSe cores for samples S1-S4: The procedure follows that reported by Manna and coworkers.[1] CdO (60 mg), ODPA (280 mg) and TOPO (3 g) were loaded in a 50 mL flask and heated under vacuum for 1 hour at 150^{o}C. After that the solution was heated under argon to 340^{o}C. At that point when the CdO already dissolved and the solution was clear and colorless 1.5 mL of TOP were injected. The temperature was allowed to recover and rise to the desired injection temperature, between 365^{o}C and 390^{o}C, when 58 mg Se in 0.4 mL TOP were injected. Different sizes of cores were obtained by modifying the injection temperature and the duration of heating after injection. For instance, the smallest cores were obtained when the injection occurred at 390^{o}C and the heating mantle was removed immediately after injection.

Synthesis of CdSe sample S5: CdO (13 mg), TDPA (62 mg) and ODE (5 mL) were loaded in a 25 mL flask and heated under vacuum at 120 ^{o}C for one hour. After that the temperature was raised to 280^{o}C for injection of 8 mg Se in 2 mL TOP. The temperature was stabilized at 240^{o}C for 45 minutes of growth. This method produces larger elongated rods depicted in Figure S1.

Synthesis of CdS QDs: The procedure followed a previous report with slight modifications.[2] In a typical synthesis 38 mg CdO, 6 mL ODE and 0.3 mL OA were placed under vacuum for 1 hour. After that the temperature was raised to 250 ^{o}C under argon, for injection of 2 mL sulfur/ODE solution (0.1 M). The temperature was allowed to recover to 250^{o}C and held for 1 minute, before heating was removed.

Synthesis of CdSe/CdS core/shell QDs: The procedure was very similar to other reports. 1.5 g of ODA and 8 mL of ODE were put under vacuum with mild heating for 1 hour. The vacuum was stopped, the system was flushed with argon and at room temperature, 100 nanomoles of clean CdSe cores, dispersed in 3 mL heptane with a few drops of octylamine were injected. The system was put under vacuum again to remove all heptane. After that the temperature was raised to 240^{o}C for alternating injections of Cd-oleate (0.1M) and Se-TOP (0.1M) with fifteen minutes intervals between injections for the first monolayer and ten minutes for the rest. The amounts injected were calculated in order to achieve a single monolayer growth per cycle.

Synthesis of CdS/CdSe core/shell QDs: The procedure also followed ref. 2. The synthesis continued from that of CdS cores, without stopping the reaction. 3 mL CdS cores were removed from the reaction for the CD experiment, before shell growth. After that the temperature was stabilized at 200^{o}C for alternating injections of Cd-Oleate (0.1 M) and Se-TOP (0.1 M) at 20 minutes intervals.

Synthesis of CdTe/CdSe QDs: CdO (26 mg), TDPA (120 mg) and 6 ml ODE were loaded in a 25 mL flask and heated under vacuum at 120 ^{o}C for one hour. Separately, 7 mg tellurium was dissolved in 0.5 g TBP and 1.5 g ODE in a glove box. The temperature of the reaction was raised to 300^{o}C under Argon, before the tellurium solution was taken out from the glove box and quickly injected. The temperature was stabilized on 250^{o}C for 30 minutes after the injection, for growth of CdTe quantum dots. Layers of CdSe were grown at 200^{o}C by drop wise addition of 0.1M Se-TOP solution, with intervals of 20 minutes between growth of monolayers.

Phase transfer procedure: The procedure was slightly modified from that described by Balaz and coworkers in their papers cited in the manuscript. An amount of clean QDs that gave an O.D of 2.5 at the band edge peak position, were dissolved in 4 mL toluene. An aqueous phase containing 8 mL L-cysteine solution (0.062 M cysteine in a pH 10.5 solution) was then mixed with the organic phase under vigorous stirring. A few drops of acetone were added to facilitate the phase mixture and the phase transfer was allowed to occur for 6 hours in the dark. After that the solution was allowed to stand for 30 minutes for the phases to separate and the bottom aqueous phase was removed. The QDs were purified using acetone/water mixtures 3/1 for the first centrifugation cycle and 8/1 for the second. The clean QDs were dispersed in 2.6 mL DI water.

Absorption and CD measurements: CD measurements were performed using an Applied Photophysics Chirascan CD spectrometer. Absorption measurements were performed using a Varian Carry 5000 spectrometer. All samples were measured in a 1 cm path length fused quartz cuvette.

Transmission electron microscopy: Images were recorded using a FEI Tecnai F20 FEG-TEM operating at 200 kV.

TEM images

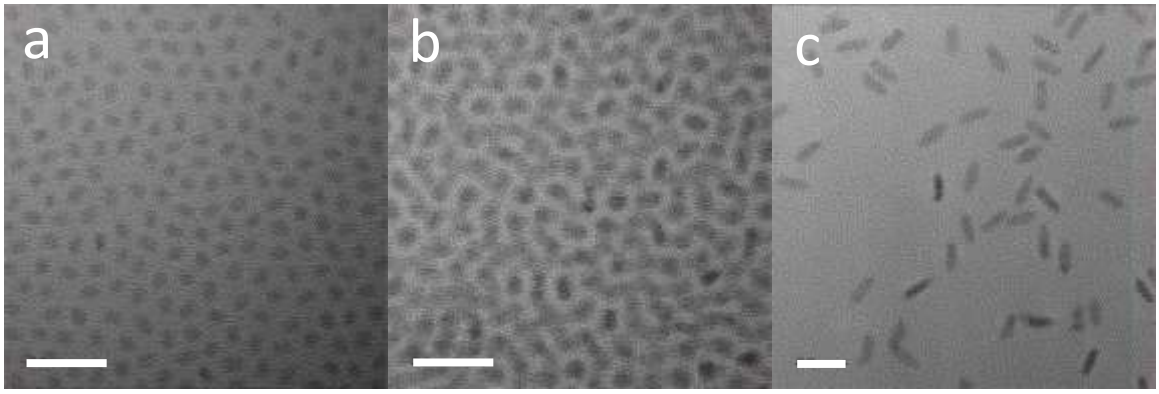

Figure S1. TEM images of CdSe samples of different sizes. All the samples are characterized by slightly elongated geometries. (a) Sample S2 in the manuscript with an average width 3±1 nm. (b) Sample S3, with an average width of 3.5±0.2nm . (c) Sample S5, that is obtained in a slightly different synthesis exhibits the highest aspect ratio, with an average width of 5.3±0.2 nm. Scale bar is 20 nm for all images.

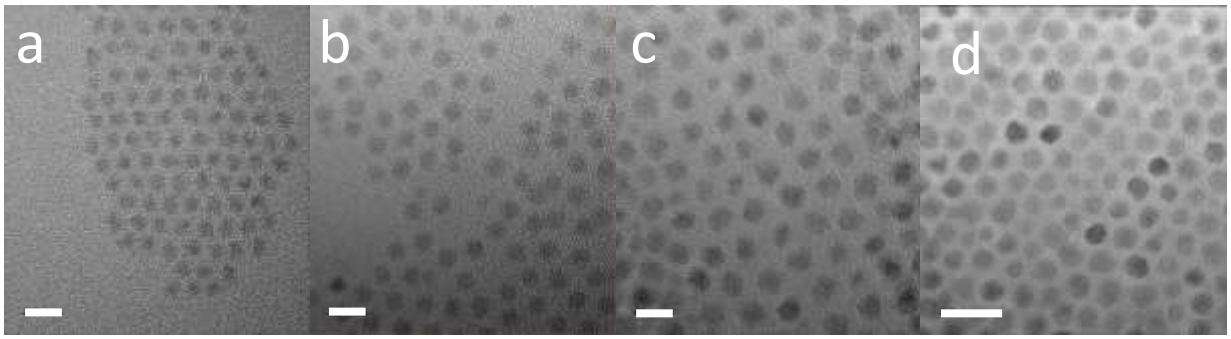

Figure S2. TEM images of CdSe/CdS core/shell QDs. Images a-d depict CdSe/CdS core/shell QDs with 0 (cores), 1, 3 and 5 monolayers of a CdS shell. The particles are with a slightly elongated shape, with an average width of 3±0.1, 3.7±0.3, 4.6±0.5 and 6.7±0.5 nm, for a-d, respectively. The scale bars represent 10 nm for (a-c) and 20 nm for (d).

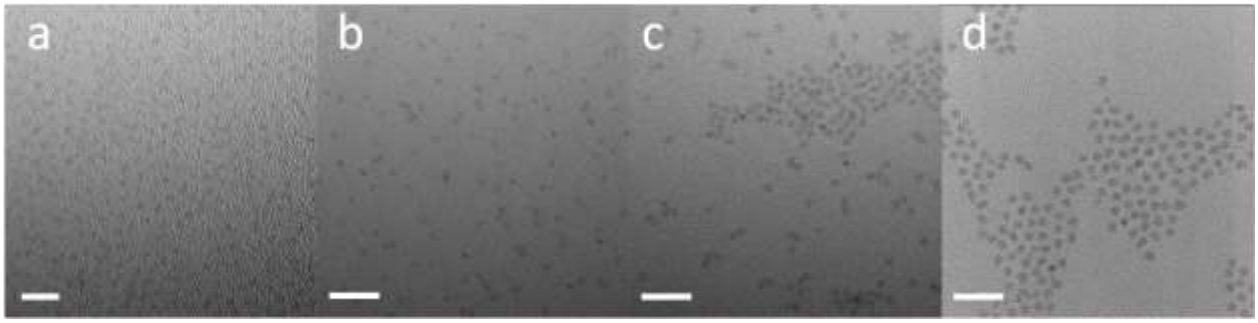

Figure S3. TEM images of CdS/CdSe core/shell QDs. Images a-d depict CdS/CdSe core/shell QDs with 0 (cores), 1, 3 and 5 monolayers of a CdSe shell. The particles' average widths for a-d are 2.8±0.1, 3.5±0.2, 4.6±0.3 and 5.6±0.4 nm, respectively. The scale bars represent 10 nm for (a) and 20 nm for (b-d).

Spectra of CdS samples

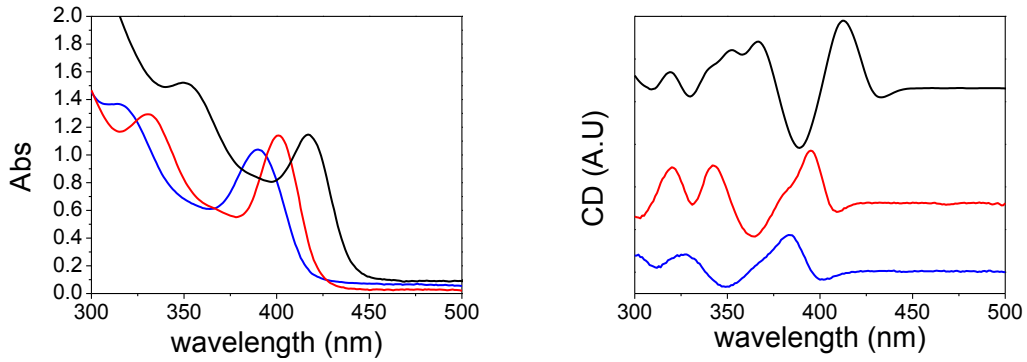

Figure S4. Absorption and CD spectra of CdS QDs. The absorption and CD of three different sizes of CdS QDs are presented. The lineshape is preserved as in the case of CdSe. The middle size is the one presented in the manuscript.

Spectral analysis

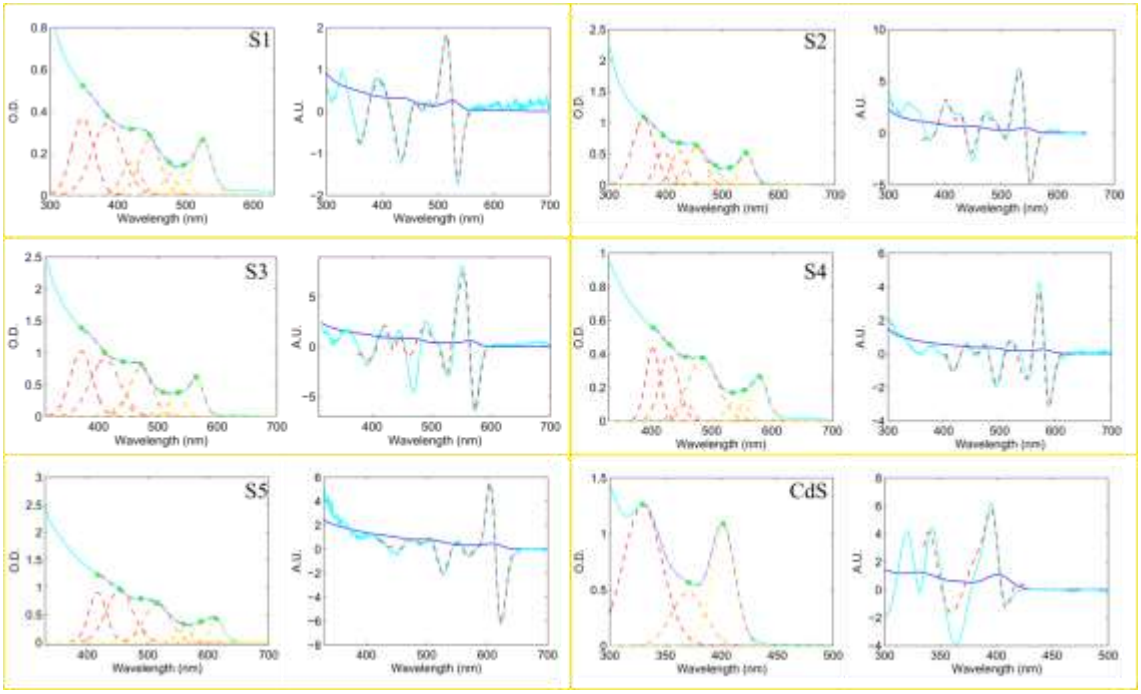

Figure S5. Results of deconvolution analysis for all the samples. This image depicts the results of the analysis presented in Figure 3 of the manuscript for all five CdSe QDs samples (S1-S5 in the manuscript), and the CdS sample presented in the manuscript (bottom right).

CD analysis:

Each excitonic level is approximated using a Gaussian function and the total absorption as a sum of Gaussians:

$$abs(\lambda) = \sum_{i=1}^{n} A_{0_i} \cdot e^{-\frac{(\lambda-\lambda_{0_i})^2}{2\cdot\sigma_i^2}}$$

This model is suitable even if energy splitting occurs as the shift $\Delta\lambda_i$ is negligible relative to λ (the absorption measurement resolution is much lower than $\Delta\lambda_i$):

$$abs(\lambda) = \sum_{i=1}^{n} \frac{A_{0_i}}{2} \cdot e^{-\frac{(\lambda-\lambda_{0_i}+\Delta\lambda_i)^2}{2\cdot\sigma_i^2}} + \frac{A_{0_i}}{2} \cdot e^{-\frac{(\lambda-\lambda_{0_i}-\Delta\lambda_i)^2}{2\cdot\sigma_i^2}} \approx \sum_{i=1}^{n} A_{0_i} \cdot e^{-\frac{(\lambda-\lambda_{0_i})^2}{2\cdot\sigma_i^2}}$$

The CD spectrum which measures the excitonic level dissymmetry resulting from the QD's interaction with its chiral ligands, is sensitive to small level shifts. Hence, the spectrum is modeled as a sum of differences between couples of Gaussians formed by small shifting from the original center Gaussians in the absorption spectrum:

$$CD(\lambda) = \sum_{i=1}^{n} A_{0_{i,l}} \cdot e^{-\frac{(\lambda-\lambda_{0_i}+\Delta\lambda_i)^2}{2\cdot\sigma_i^2}} - A_{0_{i,r}} \cdot e^{-\frac{(\lambda-\lambda_{0_i}-\Delta\lambda_i)^2}{2\cdot\sigma_i^2}} \approx$$

$$\sum_{i=1}^{n} \frac{A_{0_i}}{2} \cdot e^{-\frac{(\lambda-\lambda_{0_i}+\Delta\lambda_i)^2}{2\cdot\sigma_i^2}} - \frac{A_{0_i}}{2} \cdot e^{-\frac{(\lambda-\lambda_{0_i}-\Delta\lambda_i)^2}{2\cdot\sigma_i^2}} \approx \sum_{i=1}^{n} \Delta\lambda_i \cdot \frac{d\big(abs(\lambda)\big)}{d\lambda}$$

As $\frac{d(abs(\lambda))}{d\lambda} = \sum_{i=1}^{n} \lim_{\Delta\lambda_i\to 0} \frac{A_{0_i}\cdot e^{-\frac{(\lambda-\lambda_{0_i}+\Delta\lambda_i)^2}{2\cdot\sigma_i^2}} - A_{0_i}\cdot e^{-\frac{(\lambda-\lambda_{0_i}-\Delta\lambda_i)^2}{2\cdot\sigma_i^2}}}{2\cdot\Delta\lambda_i}$

For simplicity, a second step approximation is assumed in the calculation above in which $A_{0_{i,l}} \approx A_{0_{i,r}} \approx \frac{A_{0_i}}{2}$. This means that the amplitude for excitation with left or right circular polarizations, of each of the sub states is the same. The CD spectrum can then be written as a linear sum of derivatives of the Gaussians in the absorption spectrum:

$$CD(\lambda) \approx \sum_{i=1}^{n} \theta_{\mathrm{CD}_i} \cdot \frac{d(A_{0_i} \cdot e^{-\frac{(\lambda-\lambda_{0_i})^2}{2\cdot\sigma_i^2}})}{d\lambda}$$

This result immediately gives the energy splitting directly from the CD fit parameters $\theta_{\mathrm{CD}_i} = \Delta\lambda_i$.

To verify this calculation we check for the case of a single Gaussian:

$$abs(\lambda) = A_{0_i} \cdot e^{-\frac{(\lambda-\lambda_{0_i})^2}{2\cdot\sigma_i^2}}$$

$$CD(\lambda) = \theta_{\mathrm{CD}_i} \cdot \frac{d(A_{0_i} \cdot e^{-\frac{(\lambda-\lambda_{0_i})^2}{2\cdot\sigma_i^2}})}{d\lambda} = \theta_{\mathrm{CD}_i} \cdot -\frac{2(\lambda-\lambda_{0_i})}{2\cdot\sigma_i^2} \cdot A_{0_i} \cdot e^{-\frac{(\lambda-\lambda_{0_i})^2}{2\cdot\sigma_i^2}} \rightarrow$$

Now we look at the CD extrema points at $\lambda_{0_i} + \sigma_i$:

$$CD(\lambda_{0_i} + \sigma_i) = \theta_{\mathrm{CD}_i} \cdot -\frac{2(\lambda_{0_i}+\sigma_i-\lambda_{0_i})}{2\cdot\sigma_i^2} \cdot A_{0_i} \cdot e^{-\frac{(\lambda_{0_i}+\sigma_i-\lambda_{0_i})^2}{2\cdot\sigma_i^2}} = -\frac{\theta_{\mathrm{CD}_i}\cdot A_{0_i}}{\sqrt{e}\cdot\sigma_i} = -\Delta A \rightarrow$$

$\theta_{\mathrm{CD}_i} = \frac{\Delta A\cdot\sqrt{e}\cdot\sigma_i}{A_{0_i}} = \Delta\lambda_i$. The final result shows that the energy splitting is proportional to $\frac{\Delta A}{A}$ at the wavelength where it is maximal. This is the dissymmetry factor often used in chiroptical activity measurements. This equation directly corresponds to well-known procedures for analysis of magnetic CD in QDs (see reference 29 in the manuscript).

In terms of energy:

$$\Delta E_i = \Delta\lambda_i \cdot \frac{2\cdot h\cdot c}{{\lambda_{0_i}}^2} = \Delta\lambda_i \cdot \frac{2480}{{\lambda_{0_i}}^2}$$

More details on the fitting procedure:

Each absorption spectrum is fitted by a sum of Gaussians using least square means with fitting parameters of $(A_{0_i}, \lambda_{0_i}, \sigma_i)$. The initial guess for the center is based on the minimums of the second derivatives of the absorption spectrum, as an initial guess with tight borders. The initial values for amplitudes in the fit are estimated from the absorption at the center, and the width is approximated from the second derivative

maxima which borders between each minima. All absorption fits have high coefficients of determination: $R^2 > 0.997$.

Then, the CD spectrum is fitted by a linear combination of the derivatives of the Gaussians found by the Absorption decomposition $CD(\lambda) \approx \sum_{i=1}^{n} \theta_{\mathrm{CD}_i} \cdot \frac{d(A_{0_i} \cdot e^{-\frac{(\lambda-\lambda_{0_i})^2}{2\cdot\sigma_i^2}})}{d\lambda}$. It was found that little tweaking of the width σ_i retrieved at the first analysis step, is necessary for high agreement between the CD spectrum and the fit. This can be explained by the different broadening mechanisms associated with CD versus absorption.

Therefore, the CD spectrum fitting parameters are (θ_{CD_i}, σ_i). This results with approximation of the level splitting: $\theta_{\mathrm{CD}_i} \approx \Delta\lambda_i$.

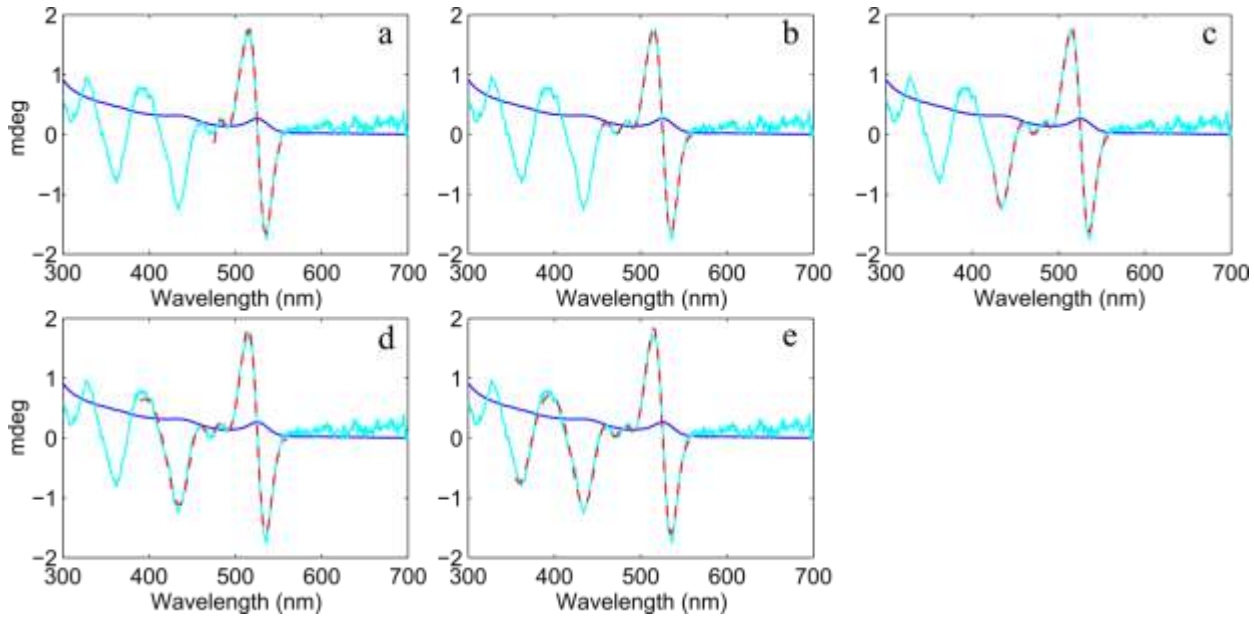

Figure S6. Analysis of CD spectra. This figure depicts the evolution of CD lineshape for sample S1 in the manuscript, with addition of higher energy excitonic transitions to the fit. The fitted CD curves using 3 (panel a), 4 (panel b) , 5 (panel c), 6 (panel d) and 7 (panel e) excitons (Gaussians) are depicted in red dashed lines. The measured CD spectra appear in cyan, and the measured absorption spectra in blue. This result is demonstrated for only one sample, but works similarly for all other samples.

Energy splitting values:

	ΔE_i (ev)							λ_{0_i}(nm)						
	7	6	5	4	3	2	1	7	6	5	4	3	2	1
S1	30	-28	84	-33	-23	-19	27.0	348	384	419	447	476	497	525
S2	-79	-56	-28	-43	-64	-26	36	361	396	423	455	488	514	543
S3	-26	-38	-42	-25	-6	-37	38	371	411	441	471	509	534	564
S4	43	15	96	28	79	-38	45	403	430	457	485	535	554	579
S5	-3	9	26	18	29	8	51	417	453	489	516	560	588	614
CdS					-65	-113	13					330	370	402

Table 1. The split in energy ΔE_i for the different excitonic states 1-7, corresponding to the Gaussians peak positions at λ_{0_i} values given on the right hand side of the table. The first five samples S1-5 are CdSe QDs, and the last sample is the CdS QDs sample presented in the manuscript. The 1-7 states are assigned for CdSe QDs in the manuscript.

	$\sigma_{i_{CD}}$							$\sigma_{i_{OD}}$						
Sample	7	6	5	4	3	2	1	7	6	5	4	3	2	1
S1	16.5	22.8	13.8	16.0	9.2	9.5	13.9	13.3	45.6	27.6	15.6	9.4	10.6	9.7
S2	32.1	15.5	9.8	15.5	22.4	8.6	8.9	19.4	13.6	13.2	15.6	11.2	10.8	11.4
S3	21.8	17.3	7.4	18.6	5.7	9.6	9.1	18.5	25.1	12.0	18.8	10.7	12.5	12.4
S4	14.3	22.5	18.5	12.3	15.5	18.0	9.0	12.0	15.5	10.5	24.5	12.0	9.0	13.8
S5	7.3	44.0	11.9	12.6	16.5	8.2	9.8	14.5	22.0	10.0	21.5	12.5	12.3	11.9
CdS					10.9	19.9	6.0					17.2	14.7	10.8

Table 2. Gaussian σ_i tweaking for the CD spectra analysis. $\sigma_{i_{CD}}$ after CD fit analysis for the different excitons and $\sigma_{i_{OD}}$ form OD analysis.

Effective mass calculations for core/shell QDs

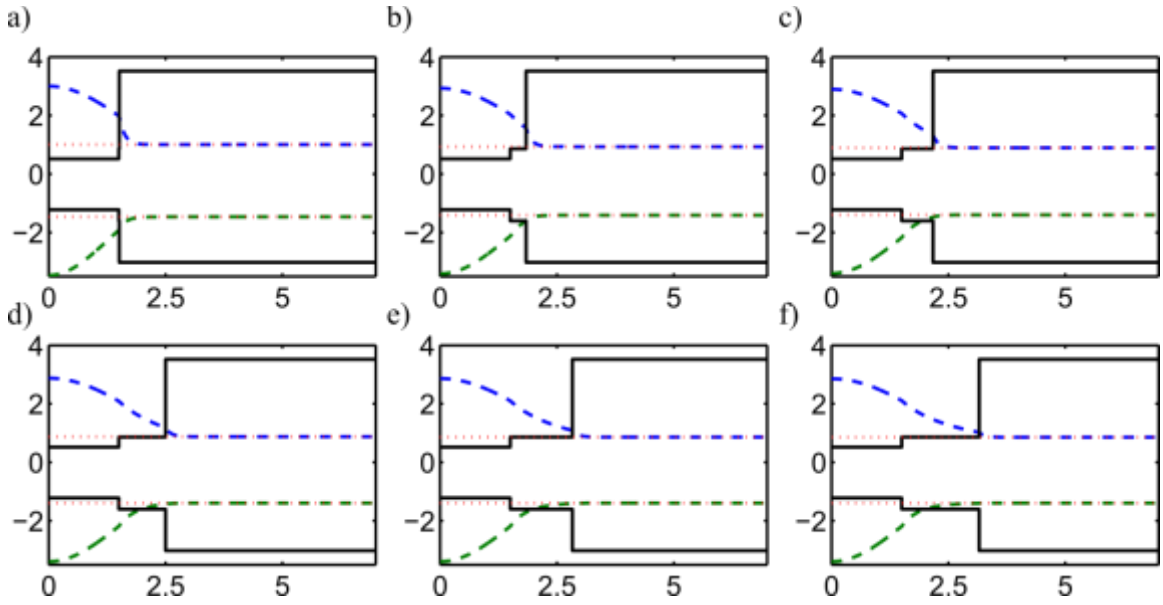

Figure S7: Diagrams depicting effective mass calculations of the wavefunctions of holes and electrons in the samples presented in Figure 4 a,b in the manuscript. The y-scales refer to the black curves which represent potential energy of the valence and conduction band edges (in eV) as function of radial distance from the center (in nm). (a) CdSe cores, (b-f) CdSe/CdS with one to five monolayers of CdS shell correspondingly. The green and blue dashed lines mark the radial hole and electron wavefunctions respectively, also plotted as a function of radial distance from the center (units on the y scale are not relevant for the wavefunction schematics). For a thick shell the hole is mostly localized in the core.

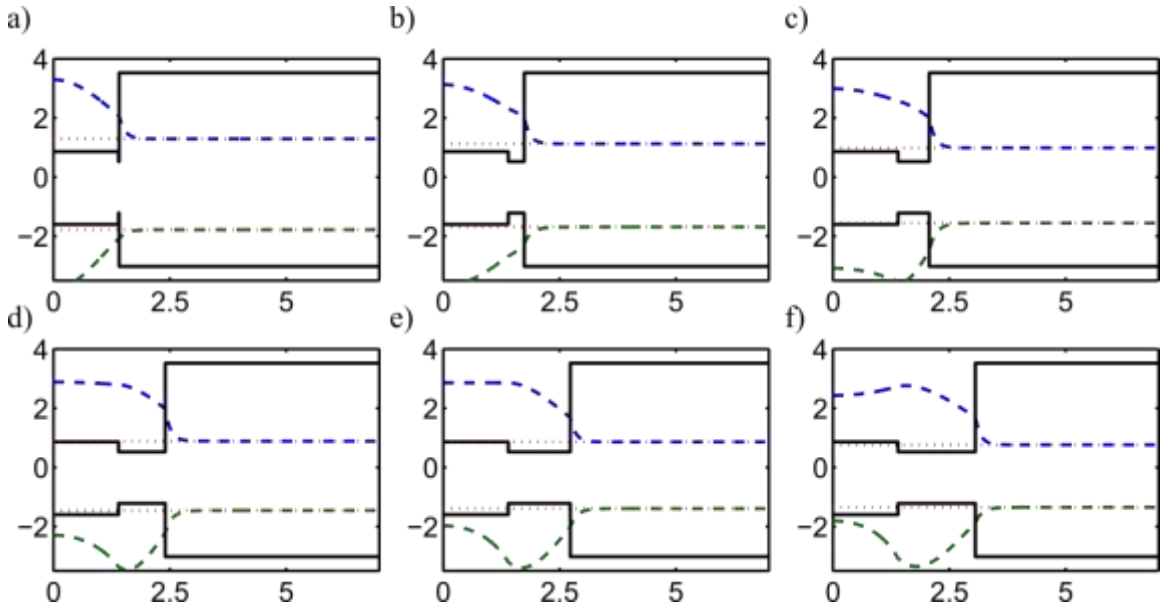

Figure S8: Diagrams depicting effective mass calculations of the wavefunctions of holes and electons in the samples presented in Figure 4 c,d in the manuscript. The y-scales refer to the black curves which represent potential energy of the valence and conduction band edges (in eV) as function of radial distance from the center (in nm). (a) CdS cores, (b-f) CdS/CdSe with one to five monolayers of CdSe shell correspondingly. The green and blue dashed lines mark the radial hole and electron wavefunctions respectively, also plotted as function of radial distance from the center (units on the y scale are not relevant for the wavefunctions schematics, and are only relevant for black potential curves). For a thick shell the hole is mostly localized in the shell.

Results for CdTe/CdSe samples

Measurements were performed on a series of CdTe/CdSe quantum dots. The bare CdTe cores were not stable during the phase transfer process, and therefore results of core/shell samples cannot be compared with the bare cores. The CD signal is very weak for all samples and seems to decay very fast with growing shell. It is already undetectable by the third monolayer of shell. This verifies the role of holes in the induction process, similarly to the results presented for CdSe/CdS samples.

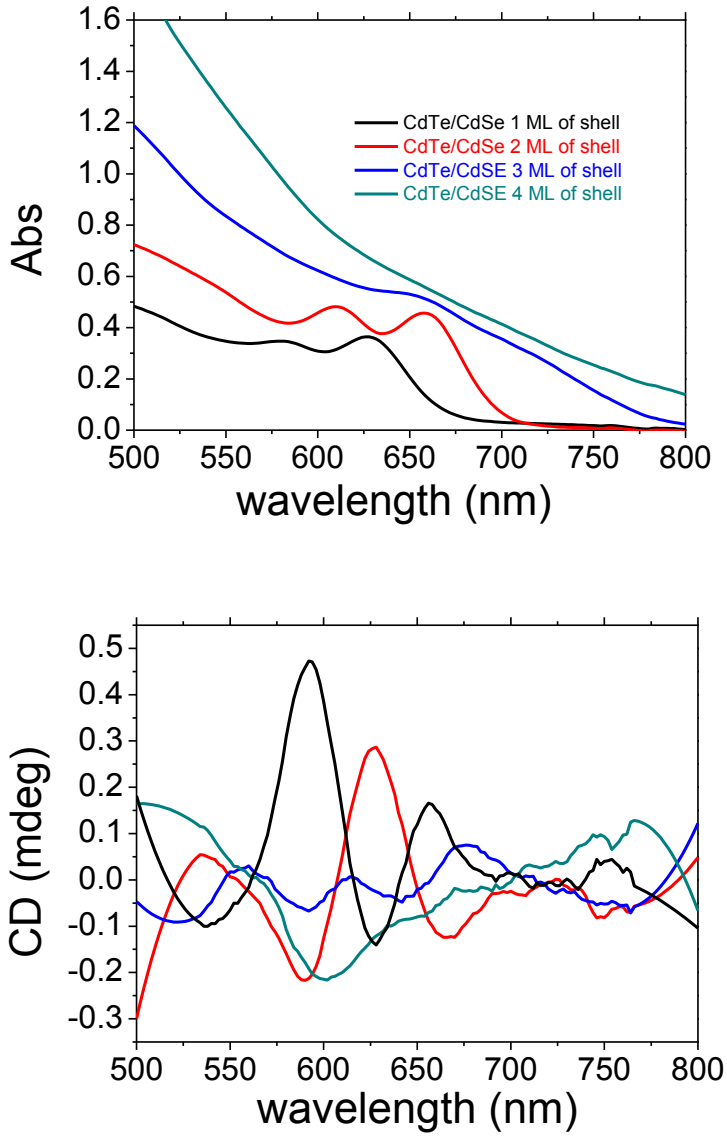

Figure S9: Absorption and CD spectra for CdTe cores (diameter 3.9 nm), with 1-4 monolayers (ML) of CdSe shell.

References

1. Carbone, L. et al. *Nano Lett.* **2007**, 7, 2942-2950.
2. Pan, Z.; Zhang, H.; Cheng, K.; Hou, Y.; Hua, J.; Zhong, X. *ACS Nano* **2012**, 6, 3982-3991.